A&A manuscript no.
(will be inserted by hand later)

Your thesaurus codes are:
08(02.13.5; 09.13.2; 13.21.3)

ASTRONOMY
AND
ASTROPHYSICS
26.7.1995

Photodestruction of PAHs in the interstellar medium

II. Influence of the states of ionization and hydrogenation

T. Allain[1,2], **S. Leach**[1], **and E. Sedlmayr**[2]

[1] Département Atomes et Molécules en Astrophysique, CNRS-URA812, Observatoire de Paris-Meudon, 92195 Meudon, France
[2] Institut für Astronomie und Astrophysik, Technische Üniversität Berlin, PN 8-1, Hardenbergstraße 36, D–10623 Berlin, Federal Republic of Germany

Received 2 February 1995; accepted 12 April 1995

Abstract. We have extended the model for interstellar polycyclic aromatic hydrocarbons (PAHs) of Allain *et al.* (1995) in order to describe ionized and partially dehydrogenated PAHs and hence provide a more realistic description of these species in the interstellar medium (ISM). When ionized and partially dehydrogenated, PAHs are less stable against photodestruction than their parent molecules. For instance, an ovalene cation with 32 carbon atoms has photodissociation rates 4 times greater than the corresponding molecule, whereas the corresponding totally dehydrogenated molecule has photodissociation rates 3 orders of magnitude greater. However, in the regions where the unidentified infrared (UIR) emission bands have been observed (reflection nebulae, planetary nebulae, HII regions, active galactic nuclei...) only PAHs with less than 50 carbon atoms may be considerably dehydrogenated. In contrast, the fraction of ionized PAHs is quite similar for all molecular sizes of PAHs but its value largely depends on the physical properties of the considered medium. A low ionization fraction is always found to be associated with relatively high hydrogen coverage of small PAHs. After taking into account these ionization and hydrogenation states we conclude that PAHs with more than 50 carbon atoms may survive the UV radiation field in the regions of the ISM where the UIR bands are observed. The smaller PAHs are all destroyed within some years in the media of high UV field which exhibit the UIR bands.

Key words: ISM:molecules – molecular processes – ultraviolet:ISM

Send offprint requests to: T. Allain

1. Introduction

Seven years after the first observations of the unidentified infrared (UIR) emission bands in the spectra of astrophysical sources (Gillet *et al.* 1977), it was proposed by Léger & Puget (1984) and by Allamandola *et al.* (1985) that these bands may be attributed to free polycyclic aromatic hydrocarbons (PAHs). The emission bands are mainly observed in regions associated with an intense UV radiation field (reflection nebulae, planetary nebulae, HII regions, active galactic nuclei...) and ultraviolet absorption is therefore generally thought to be the excitation process of PAHs. Since the emission band at 3.3 μm has also been seen in the diffuse medium (Giard *et al.* 1988), PAHs could be an ubiquitous component of the interstellar medium (ISM).

Using the relative intensities of the spectra of the UIR bands and models for the excitation of PAHs, it is possible to estimate the molecular size of interstellar PAHs (Allamandola *et al.* 1987, 1989). Geballe *et al.* (1989) have for instance estimated that in the Orion Bar and the Red Rectangle PAHs should contain 15 – 20 carbon atoms, and Woodward *et al.* (1989) obtained an estimation of 13 – 27 carbon atoms in the case of NGC 7027. These results have led Duley & Jones (1990) to suggest that PAHs such as naphthalene, anthracene and tetracene are responsible for the emission of the UIR bands. These propositions have been recently questioned by the experimental results of Jochims *et al.* (1994a) who have shown that only PAHs having more than 30 – 40 carbon atoms are expected to survive the interstellar radiation field. A theoretical study based on these results by Allain *et al.* (1995) (hereafter paper I) has concluded that the photodissociation rates of PAHs molecules having less than 50 carbon atoms are larger than the rate for accretion of carbon in the regions where the UIR bands are observed, and that these PAHs are destroyed within some years in the regions of high UV radiation field.

The photodissociation rates calculated in paper I have been obtained for fully hydrogenated PAH molecules. However, interstellar PAHs are thought to be ionized and partially dehydrogenated. (Léger & d'Hendecourt 1985; van der Zwet & Allamandola 1985; Omont 1986; Tielens *et al.* 1987; Allamandola *et al.* 1989; Geballe *et al.* 1989; Léger *et al.* 1989a,1989b; Verstraete *et al.* 1990). Cations and partially dehydrogenated PAHs are possibly less stable against photodissociation and it is the aim of this paper to investigate their photodissociation rates in the regions showing the UIR bands. These rates are calculated in the first section. In the next section, the states of ionization and dehydrogenation of PAHs in these environments are estimated and, finally, the implications for the molecular size of interstellar PAHs are discussed.

2. Rates of photodissociation of dehydrogenated PAHs and PAH cations

In paper I we have developed a model in order to estimate the rates of photodissociation of PAH molecules in UV exposed regions. We propose here some modifications to take into account PAH cations and dehydrogenated PAHs. Using this modified model we calculate the rates for photodissociation of ionized and partially dehydrogenated PAHs.

2.1. Extension of the model to PAH cations

Léger & d'Hendecourt (1985), Omont (1986) and Verstraete *et al.* (1990) have shown that in some astrophysical environments a large fraction of PAHs are ionized. It is therefore worthwhile estimating the rates of photodestruction of PAH cations. Following the same approach as in paper I, we have considered the UV and visible absorption cross–sections of PAH cations as well as their rates of UV, visible and IR luminescence, ionization and photodissociation.

The UV and visible absorption spectra of naphthalene, pyrene, perylene and coronene cations (Salama & Allamandola 1991,1992; Lee & Wdowiak 1993a) have been recently measured in various matrices showing some differences with the spectra of their neutral precursors, especially the development of an absorption continuum. Since it is not yet clear whether the experimental set–up is responsible for this continuum, we do not take it into account in our calculations. Moreover, when no data have been found, we have assumed that the cation has the same UV absorption cross–section as its parent molecule. For large PAHs the expression of Verstraete & Léger (1992), obtained by a theoretical calculation based on the properties of graphite, was used to determine the absorption cross–section.

The electronic levels of PAH cations are doublets and quartets. Unfortunately, the results available on transition rates of PAH cations are relatively scarce and make their study difficult for PAHs larger than $C_6H_6^+$. Nevertheless, Leach (1987) has shown that internal conversion (IC) to the electronic ground state D_0 dominates, leaving all the excitation energy in the form of vibrational energy of the D_0 state. In our model for PAH cations we therefore neglect visible fluorescence and phosphorescence. The PAH cations have hence only one route for deactivation via luminescence, namely IR emission. These emissions may however differ from those of the parent molecule in a way that is still unknown for most PAHs. Dunbar (1986) has for instance reported that the infrared emission rates of the benzene cation are 4 – 5 times faster than those of neutral benzene. Few other studies of IR relaxation of PAH cations have been found in the literature. We therefore adopt the same values as those of the corresponding molecule. There are also few data about the IR frequencies of PAH cations. Klippenstein *et al.* (1993) have tabulated the frequencies of the benzene molecule and cation in their study of benzene cation dissociation. The two series of vibrational frequencies are quite similar and we assume that this is also the case for larger PAHs.

Concerning the ionization of PAH cations we use the values of the ionization potential (IP) from Leach (1986) and Tobita *et al.* (1994) and assume a linear increase of the yield of ionization with the internal energy of the PAH cation as proposed by Jochims *et al.* (1994b). The IP of PAH cations are all about 13 eV and the contribution of ionization of cations in the 2.8 –13.6 eV range of interest for us is always found to be negligeable.

In paper I we have used the experimental results of Jochims *et al.* (1994a) to describe the processes of photodissociation of PAHs. These results have been obtained for PAH cations. In paper I we have however used them for molecules following Jochims *et al.* (1994a) who argue that the rates are valid for both molecules and cations because they have similar intramolecular dynamics. The experimental rates are well reproduced by the RRK theory which provides the following expressions:

$$\begin{aligned} k(E) &= k_0\left(1 - \frac{E_0}{E}\right)^{s-1} && \text{for } E > E_0\ , \\ k(E) &= 0 && \text{for } E \leq E_0\ , \end{aligned} \qquad (1)$$

where E is the internal energy of the molecule and s the number of degrees of freedom over which the energy E can be distributed. In our case we assume that all degrees of freedom are involved; this corresponds to $s = 3N - 6$ where N is the number of atoms of the molecule. E_0 and k_0 are two constants determined by fitting the results of the experiment and are given in Table 1 for the loss of H, H_2 and C_2H_2.

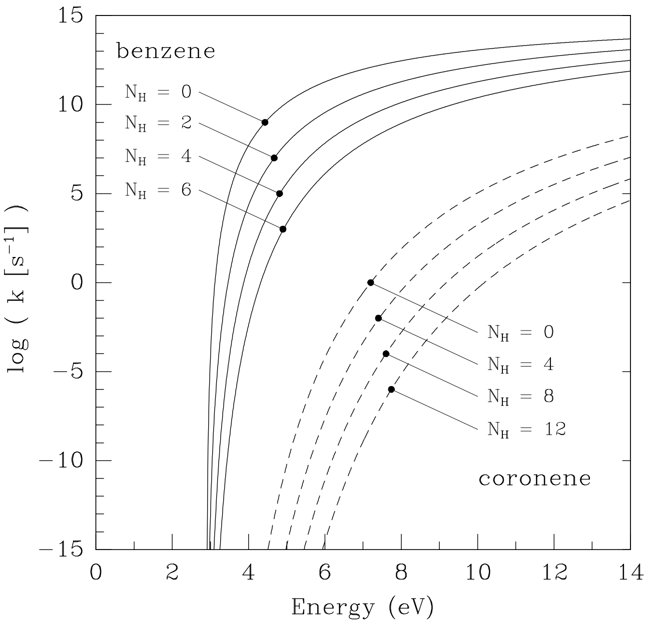

Fig. 1. Rates of photodissociation for the loss of carbon from fully and partially dehydrogenated benzene and coronene as a function of the internal energy.

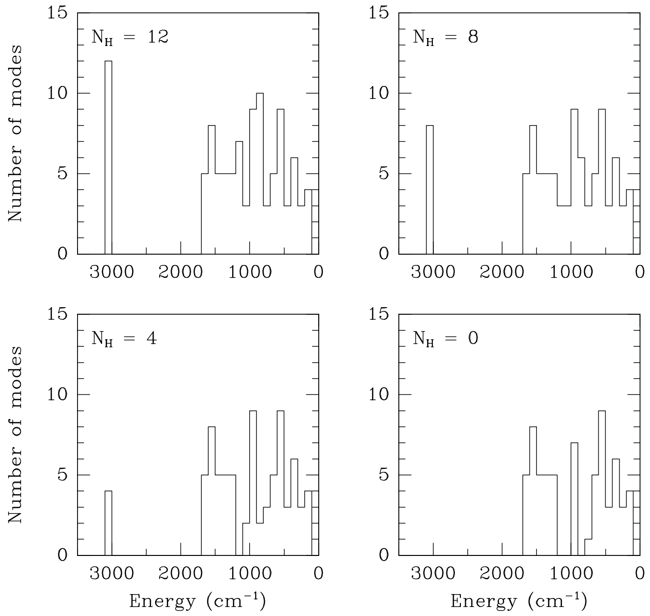

Fig. 2. Energy distribution of vibrational modes (packed in 100 cm^{-1} bins for representational convenience) for coronene (N_H=12) and for some dehydrogenated coronene molecules.

Table 1. Parameters for the RRK expression

loss channel	$E_0(eV)$	$k_0(s^{-1})$ $^{(a)}$
H	2.8	1 (16)
H_2	2.9	1 (16)
C_2H_2	2.9	1 (15)

(a) Powers of ten are written inside the brackets

2.2. Extension of the model to partially dehydrogenated PAHs

In astrophysical conditions, PAHs are thought to be partially dehydrogenated (van der Zwet & Allamandola 1985; Tielens *et al.* 1987; Allamandola *et al.* 1989; Geballe *et al.* 1989; Léger *et al.* 1989a,1989b). Unfortunately, there is little knowledge concerning the physical and chemical properties of dehydrogenated PAHs and we have had to make some assumptions to integrate partially dehydrogenated PAHs into our model.

For these species we first assume that photochemical processes of dissociation are still correctly described by the RRK theory and that the same constants E_0 and k_0 can be used for this purpose. In the case of a highly dehydrogenated PAH we also assume that the abstraction of carbon still happens via the loss of two neighbouring carbon atoms connected by a double bond. We therefore use the constants E_0 and k_0 presented in Table 1 for partially and totally dehydrogenated PAHs. We have plotted in Fig. 1 the rates calculated from Eq. (1) for the loss of an acetylene-like molecule from benzene and coronene in various hydrogenation states. From Fig. 1 it is evident that partially dehydrogenated PAHs are less stable than the corresponding non dehydrogenated molecules. More quantitatively, it is shown that the rates for totally dehydrogenated PAHs can be up to 5 orders of magnitude greater than the corresponding rate for the non dehydrogenated molecules. The physical explanation is that partially dehydrogenated PAHs have fewer vibrational modes over which they can redistribute their internal energy, so that the probability that this energy may be found in the modes corresponding to the potentially broken bonds is therefore higher.

The vibrational modes of PAHs are directly affected by the loss of hydrogen atoms. In paper I we have shown that this may have an influence on the Einstein coefficients of IR emissions (see relations (7), (8) and (9) of paper I) and on the processes related to the density of states (relations (2) and (13) of paper I). To estimate these modifications we use the same approach as Léger *et al.* (1989b) when they calculated the specific heat of dehydrogenated PAHs. A free molecule with N atoms has $3N-6$ vibrational modes. As the number of hydrogen atoms decreases, we progressively withdraw from the distribution the modes attributed to the hydrogen atom motions (3.34 μm, 8.6

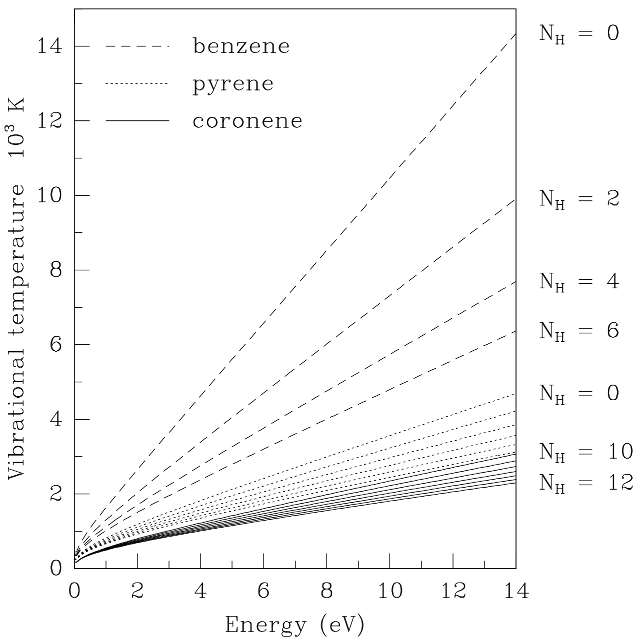

Fig. 3. Evolution of vibrational temperature with internal energy for small PAHs and their partially dehydrogenated molecules (only PAHs with an even hydrogen number N_H are represented; at a given energy these temperatures decrease with N_H).

μm, 11.3 μm) and assume that the remaining modes are not perturbed and that they have the same Einstein coefficients as those of the corresponding non dehydrogenated molecule. Figure 2 shows the evolution of the distribution of the vibrational modes as a function of the loss of hydrogen atoms for a molecule of coronene. To have an idea of the effect of dehydrogenation on the physical behaviour of PAHs, in Fig. 3 we have plotted the vibrational temperature T^* of some PAHs and of the corresponding dehydrogenated species. This temperature is defined by assuming complete energy distribution between all normal modes and consequently the following expression for the internal energy:

$$E = \sum_{i=1}^{3N-6} \frac{h\nu_i}{\exp\left(\frac{h\nu_i}{kT^*}\right) - 1} , \quad (2)$$

where N is the number of atoms in the species and ν_i the frequency of the mode i. It is clear from Fig. 3 that only the very small molecules have markedly different behaviour when they are dehydrogenated, which is not surprising because their hydrogen to carbon ratios, $N_{\rm H}/N_{\rm C}$, are larger. Coronene molecules are not very sensitive to a change of the number of hydrogen atoms and this trend surely pertains for larger PAHs. For these PAHs we therefore do not take into account the modifications of their IR properties as precisely as explained above. We only scale the Einstein coefficients of the 3.3, 8.6 and 11.3 μm IR emissions from Léger *et al.* (1989b) to the number of C – H bonds. For the sake of simplicity we have also neglected the variations of the emissions with the sites of the remaining hydrogen atoms. Léger *et al.* (1989b) and Allamandola *et al.* (1989) have indeed shown that solo, duo and trio hydrogen atoms may have various frequencies.

The UV absorption cross–section probably undergoes some changes due to the loss of hydrogen atoms. We make the following correction by considering the modification of the geometrical cross–section:

$$\sigma^{\rm UV\ abs}(N_{\rm H}) \simeq \sigma^{\rm UV\ abs}(N_{\rm H}^{\circ})\ \frac{2.5N_{\rm H}\ +\ 8N_{\rm C}}{2.5N_{\rm H}^{\circ}\ +\ 8N_{\rm C}} , \quad (3)$$

where $N_{\rm H}$ and $N_{\rm C}$ are the number of hydrogen and carbon atoms of the PAH, respectively, and $N_{\rm H}^{\circ}$ the number of hydrogen atoms of the corresponding non dehydrogenated molecule. To establish Eq. (3) we have used the relation of Omont (1986) for the radius of the PAH carbon skeleton

$$a = 0.9\ N_{\rm C}^{1/2}\ \text{Å} \quad (4)$$

and a typical length for a the C–H bond in a PAH equal to 1.077 Å (Pulay *et al.* 1981). Concerning the other physical processes of partially dehydrogenated PAHs: ionization, fluorescence, phosphorescence, internal conversion, we use the properties of the parent molecules presented in the model of paper I because of the lack of data and of the impossibility to make appropriate corrections. As these properties involve mainly the carbon skeleton of the PAHs we should not commit a large error with this assumption. The error is likely to be smaller for the larger PAHs.

2.3. Photodissociation rates of PAH cations and partially dehydrogenated molecules

As in paper I, we obtained the rate of photodissociation by integrating the corresponding cross–section over the energy available in the ISM. The photodissociation cross–section for the loss of carbon for instance can be calculated according to:

$$\sigma^{\rm C}(E) = \sigma^{\rm UV\ abs}\ \frac{k^{\rm C}(E)}{\sum k_i} , \quad (5)$$

where $\sigma^{\rm UV\ abs}$, $k^{\rm C}$ and $\sum k_i$ represent the UV absorption cross–section, the rate of photodissociation for the loss of carbon from Eq. (1) and the sum of all the rates for the processes occuring at energy E (luminescence, ionization, dissociation), respectively. Calculating the following integral:

$$k^{\rm p} = \int_{E=E_0}^{E=13.6eV} \sigma^{\rm p}(E)\ \chi\ N(E)\ dE \quad (6)$$

for a given PAH provides the rate of process (p) in the ISM. In Eq. (6) $N(E)$ represents the mean UV photon flux of the ISM at photon energy E, for which we have

Table 2. Photodissociation rates for hydrogen loss from PAH cations and dehydrogenated molecules in the interstellar field of Gondhalekar *et al.* (1980) (unit = year^{-1})

PAH	cation		$\alpha_H = 0.5$		$\alpha_H = 0.25$	
	H loss	H_2 loss	H loss	H_2 loss	H loss	H_2loss
benzene	1.1 (-1)	6.2 (-2)	8.0 (-2)	5.2 (-2)	1.3 (-1)	-
anthracene	1.7 (-1)	6.4 (-2)	1.5 (-1)	5.5 (-2)	2.9 (-1)	9.2 (-2)
pyrene	1.1 (-1)	4.4 (-2)	1.6 (-1)	5.0 (-2)	2.0 (-1)	6.7 (-2)
coronene	1.3 (-1)	4.1 (-2)	1.0 (-1)	3.3 (-2)	1.3 (-1)	4.4 (-2)
ovalene	2.2 (-2)	6.0 (-3)	3.2 (-2)	9.4 (-3)	5.7 (-2)	1.8 (-2)
PAH 50 C	2.7 (-8)	4.2 (-9)	6.7 (-6)	1.4 (-6)	1.7 (-4)	3.9 (-5)
PAH 100 C	1.4 (-25)	4.5 (-27)	2.3 (-22)	1.0 (-23)	2.2 (-20)	1.2 (-21)

Table 3. Photodissociation rates for carbon loss from PAH cations and partially dehydrogenated molecules in the interstellar field of Gondhalekar *et al.* (1980) (unit = year^{-1})

	PAH	cation	$\alpha_H = 0.5$	$\alpha_H = 0$
benzene	4.7 (-3)	6.2 (-3)	5.2 (-3)	1.4 (-1)
anthracene	6.0 (-3)	6.4 (-3)	5.5 (-3)	4.2 (-1)
pyrene	2.2 (-3)	4.4 (-3)	5.0 (-3)	2.8 (-1)
coronene	1.4 (-3)	4.1 (-3)	3.3 (-3)	2.0 (-1)
ovalene	1.5 (-4)	6.0 (-4)	9.4 (-4)	6.7 (-2)
PAH 50 C	1.1 (-10)	4.2 (-10)	1.4 (-7)	1.5 (-4)
PAH 100 C	1.0 (-28)	4.5 (-28)	1.0 (-24)	1.6 (-20)

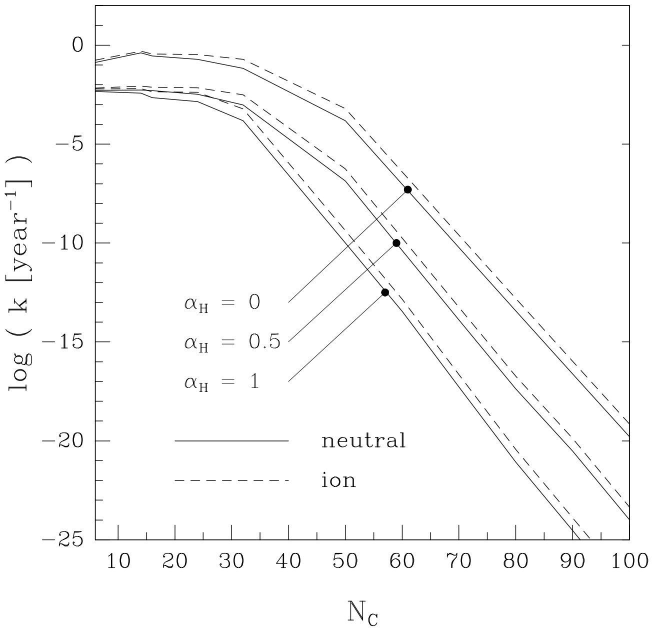

Fig. 4. Rates of photodissociation for the loss of carbon from PAH cations and partially dehydrogenated molecules as a function of the size of the PAH.

used the data of Gondhalekar *et al.* (1980) in the range 4.5 – 13.3 eV and of Mathis *et al.* (1983) for the extension over 2.8 – 13.6 eV. χ is a scaling factor used to describe the high radiation fields of the regions showing the UIR bands.

The results concerning the photodissociation of hydrogen from PAH cations and partially dehydrogenated PAH molecules are presented in Table 2. The results we have obtained for the loss of carbon are in Table 3 and have been plotted in Fig. 4 as a function of the PAH size. To simplify the discussion we have defined the hydrogen coverage of a molecule by the relation:

$$\alpha_H = \frac{N_H}{N_H^\circ} , \tag{7}$$

where N_H is the number of hydrogen atoms borne by a PAH and N_H° the number of hydrogen atoms of the corresponding non dehydrogenated PAH. When we discuss the case of a PAH with a given value of α_H, the number of hydrogen atoms of the PAH is equal to $\mathrm{INT}(\alpha_H N_H^\circ)$ where $\mathrm{INT}(x)$ represents the integer part of x.

With the results of Tables 2 and 3 and Fig. 4 we find that PAH cations are less stable than their parent molecules against photodissociation. The explanation of this behaviour is that PAH cations cannot lose as much absorbed energy through ionization as easily as the neutrals because of their higher values of ionization potential. However, the difference with the rates of the neutrals is relatively constant for all PAHs and never much larger than an order of magnitude. In the case of dehydrogenated PAHs, the situation is totally different and we observe a slightly increasing difference with the molecular size up to 8 orders of magnitude of difference for a PAH having 100 carbon atoms.

3. States of ionization and dehydrogenation of PAHs in astrophysical environments

Because of the variations of the photodissociation rates of PAHs with the ionization and dehydrogenation states, it is necessary to know the ionization fraction and the hydrogen coverage of PAHs in a given astrophysical medium in order to precisely estimate the rates for photodissociation. We therefore discuss in this section the rates of the processes governing the physical state of PAHs, and determine the state of ionization of PAHs by balancing the processes for ionization and electron recombination, and in a similar way the state of dehydrogenation by balancing the processes for hydrogen loss and hydrogenation.

3.1. Rates for the calculations

3.1.1. Rates of ionization and of electron recombination of PAHs

The rates of ionization have already been calculated in paper I for PAH molecules in a Gondhalekar *et al.* (1980) radiation field. The values for PAH ionization rates in the ISM slightly increase with the molecular size but remain about 10^{-9} – 10^{-8} s^{-1} for all PAHs. For partially dehydrogenated PAHs, the model presented in Sect. 2.2 leads to a small diminution due to the decreasing absorption cross–section (see Eq. (3)). On the other hand, the rates of ionization of PAH cations we have estimated are all lower than 10^{-10} s^{-1} and we therefore do not consider doubly charged PAHs in the following discussion, although it is thought that destruction of PAHs may also occur via double ionization in the ISM (Leach 1986; Leach *et al.* 1989).

The reverse process of ionization is recombination with an electron, for which there are only few experimental results. Recent measurements have been performed by Abouelaziz *et al.* (1993) for the electron recombination of benzene and naphthalene cations at 300 K. They obtained values of 1.10^{-6} cm^3 s^{-1} for $C_6H_6^+$ and 3.10^{-7} cm^3 s^{-1} for $C_{10}H_8^+$. Assuming a $T^{-1/2}$ dependence (Abouelaziz *et al.* 1993) one can deduce an expression for the recombination rate over the temperature range of interest in astrophysics. For small PAHs electron recombination is a dissociative process (Abouelaziz et al. 1993). This is probably not the case for larger PAHs which can be stabilized after the capture process by conversion of excess electronic energy into vibrational modes, with increasing probability as the number of internal modes rapidly increases with size. However, we have not found in the literature any systematic study of the dissociative recombination of PAHs with size. We have therefore not considered it here as a destructive process and leave to the future a study of the competition between electron dissociative recombination and photodestruction for small PAHs cations in the ISM.

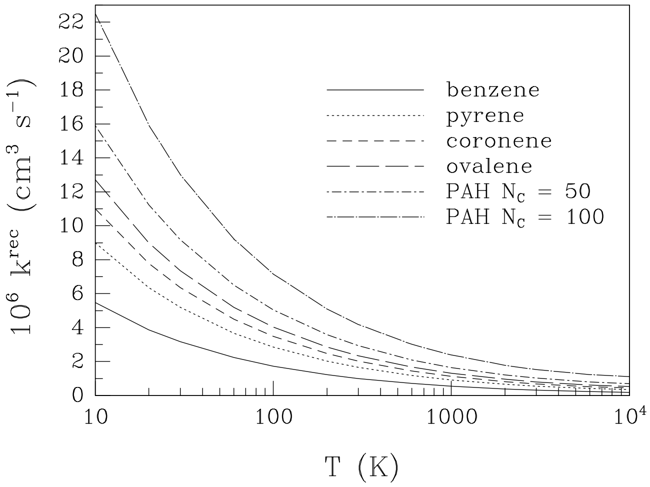

Fig. 5. PAH cation–electron recombination rates for various PAHs as a function of temperature.

For larger PAH cations no experimental values are available in the literature. We therefore follow the proposition of Léger & d'Hendecourt (1985) and Omont (1986) and use the approach of Spitzer (1978) in order to describe the recombination of an electron of speed v with a spherical particle of radius a bearing a single elementary charge $e(>0)$. From the conservation of angular momentum one easily deduces:

$$\sigma^{\rm rec} = P\ \pi a^2 \left(1\ +\ \frac{eU(a)}{1/2 m_{\rm e} v^2}\right)\ , \qquad (8)$$

where m_e is the electron mass, $U(a) = e/a$ the electronic potential at $r = a$ and P the sticking probability for recombination. The recombination rate is then obtained by averaging over a Maxwellian distribution of velocities.

$$\begin{aligned} n_{\rm e}\ k^{\rm rec}\ &=\ n_{\rm e}\ < v\sigma^{\rm rec} > \\ &=\ n_{\rm e}\ P\ \pi a^2 \left(\frac{8 k_{\rm B} T}{\pi m_{\rm e}}\right)^{1/2} \left(1\ +\ \frac{2e^2/a}{k_{\rm B}T}\right)\ , \qquad (9) \end{aligned}$$

where n_e is the electron density and k_B the Boltzmann constant. Verstraete *et al.* (1990) have shown that such an expression obtained for a sphere-shaped particle is still valid for a disk-shaped molecule of radius a if one introduces a factor of 0.8. We furthermore use the relation (4) (Omont 1986) for the radius of a PAH molecule containing N_C carbon atoms. We then deduce the value of P by ajusting the relation (9) to the experimental value of Abouelaziz *et al.* (1993) in the case of the benzene cation at 300 K (because of the geometry of the naphthalene cation, its molecular radius is not correctly described by Eq. (4) and we therefore do not use it to determine P). One hence obtains the value 0.30 for P. This value is in good agreement with the proposition of several ten percent by Omont (1986). In so doing one finally obtains numerically:

$$n_e\, k^{\rm rec} = 2.13\ 10^{-6}\ n_e\ N_{\rm C}^{1/2}\ T^{-1/2} \left[1 + 3.82\ 10^{-3}\left(\frac{T}{100}\right)\left(\frac{N_{\rm C}}{50}\right)^{1/2}\right] {\rm s}^{-1}\ . \quad (10)$$

Figure 5 represents the evolution of the recombination rate as a function of the temperature for various PAH cations. This figure shows that the rate of recombination increases with the molecular size but decreases with the temperature in the range of size and temperature of interest for the present investigation.

3.1.2. Rates for hydrogenation and for loss of hydrogen of PAHs

The rates for photoabstraction of hydrogen particles have been calculated for PAH molecules in paper I and are presented in Table 2 for cations and for partially dehydrogenated PAHs.

Lee and Wdowiak (1993b) have proposed that hydrogenation of PAHs could lead to a conversion from aromatics to aliphatic compounds. They have indeed carried out electrical discharge experiments involving hydrogen and naphthalene and shown that at least one ring of the naphthalene molecule was broken and saturated. However, the experiment is still purely qualitative and involves plasma conditions. Furthemore, the experimental value of 0.5 torr for the gas pressure is very high compared with interstellar conditions. In our calculation we have therefore not considered the reactions of PAH saturation via hydrogenation in the ISM.

The hydrogenation rate has been adapted from Frenklach *et al.* (1985) for neutral radical PAHs (rate coefficient of their reaction (21) equal to $1.7\ 10^{-11}{\rm cm}^{-3}$ molecule^{-1} s^{-1}). For the ionized species we follow the propositions of Tielens *et al.* (1987) and Allamandola *et al.* (1989) and assume a collision rate given by the Langevin rate constant ($\simeq 10^{-9}$ cm^3 s^{-1}) and, in the absence of experimental data, a reaction probability equal to unity. There is little knowledge about the temperature dependence of reaction rates for radiative association reactions. Some experimental results suggest that radiative association reactions are most effective at low temperatures. For the rates of rehydrogenation we have found no data in the literature and have assumed no temperature dependence.

However, the hydrogenation reaction competes with chemical attack by hydrogen atoms which may prove important at high temperature. Since data for chemical attack of large PAHs and dehydrogenated PAHs atoms are not available we use the kinetic data of the reaction with benzene.

$$C_6H_6 + H\bullet \longrightarrow C_6H_5\bullet + H_2\ . \quad (11)$$

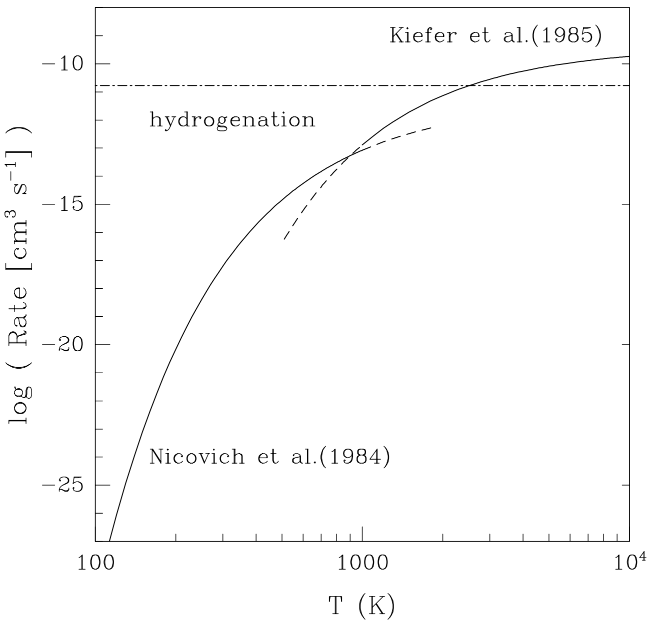

Fig. 6. Hydrogenation and abstraction rates for reaction of a benzene molecule with an hydrogen atom as a function of temperature.

Following Frenklach and Feigelson (1989) we use for the rate of this reaction the results of Kiefer *et al.* (1985) for temperatures above 1000 K and the chemical rate of Nicovich & Ravishankara (1984) for lower temperatures. These rates take Arrhenius expressions:

$$\text{for} \quad T \geq 1000\ \text{K}, \quad (12)$$
$$k^{\rm abs} = 4.15\ 10^{-10}\ \exp\left(-\frac{8060}{T}\right)\ {\rm cm}^3\ {\rm s}^{-1},$$
$$\text{for} \quad T < 1000\ \text{K},$$
$$k^{\rm abs} = 5\ 10^{-12}\ \exp\left(-\frac{4080}{T}\right)\ {\rm cm}^3\ {\rm s}^{-1}.$$

For partially dehydrogenated PAHs we also use these rates but correct them by the factor $N_{\rm H}/N_{\rm H}^{\rm o}$ which accounts for the number of peripheric hydrogen atoms $N_{\rm H}$ (this factor ensures that no abstraction can occur for fully dehydrogenated PAHs). Due to the lack of data we furthermore use the previous form of the rate of hydrogen abstraction for PAH cations, for which we indeed multiplied the rate by a factor such that the ratio of abstraction to hydrogenation is the same as for neutral PAHs. Moreover, all the previously discussed rates have been used for PAHs larger than benzene ($N_{\rm C} > 6$) by correcting with a factor $\sqrt{(N_{\rm C}/6)}$ so as to account for the increase of the collision cross–section with PAH size.

However, in many astrophysical media where the characteristic PAH emission bands are observed, the UV-field can ionize hydrogen atoms so that the predominant species is there H^+. It has indeed been observed by Woodward *et al.* (1989) in the case of NGC 7027 that the emission of the 3.3 μm band is present both inside and outside of the HII region.

Moreover, Giard *et al.* (1994) have proposed that H^+ sputtering could be responsible for the destruction of PAHs at the ionization front. However, no experimental results on H^+ chemisputtering of PAHs are available in the literature. Barlow & Silk (1977) and Draine (1979) have discussed this process for graphite and obtained contradictory results leading to a difference of four orders of magnitude for the yield of the process. As stated by Omont (1986) no definite conclusion for the destruction of PAHs by H^+ sputtering can be drawn yet. We have therefore not taken it into account for the present calculation.

There are unfortunately no experimental or theoretical results concerning the reactions of PAHs with H^+. According to Omont (1986) when a proton H^+ arrives near a PAH, it induces on the PAH a negative charge with which it interacts in such a way that the proton is neutralized when reaching a sufficiently small distance. Therefore, we use for the rates of reactions between PAH and H^+ the rates we have obtained for reactions between PAH cations and hydrogen atoms. Moreover, we logically consider no reaction between PAH cations and H^+ because of the Coulomb repulsion.

Figure 6 shows the rates of rehydrogenation and chemical attack for a benzene molecule. Clearly, hydrogenation has a rate higher than chemical hydrogen abstraction for values of the temperature lower than 2000 K. We assume that this is also the case for all PAH molecules and cations. In the media where the UIR bands have been observed the temperature is rarely greater than 2000 K and therefore under these conditions hydrogenation should be more effective than chemical hydrogen abstraction.

3.2. Equilibrium of ionization and of hydrogenation in the ISM

3.2.1. Existence and description of the equilibrium

For an ensemble of PAHs, we consider equilibrium of ionization and of hydrogenation states to exist when ionization of PAHs is balanced by electron recombination and hydrogen abstraction by hydrogenation. For the calculations, we assume that the ensemble of PAHs is immersed in a medium characterized by the hydrogen and electron densities, the temperature and the radiation field, and that these parameters are not perturbed by the processes involving PAHs. The rates describing these processes remain therefore unchanged in the calculation. Moreover, ionization, hydrogen abstraction and recombination with electrons and hydrogen are specific to each type of PAH. Thus a separate description of the equilibrium is required for each type of PAH.

However, such an equilibrium can be reached only in media where the time for destruction of PAHs is greater than the time needed to establish the equilibrium. The most efficient process of destruction in the media we investigate is photodestruction via the loss of an acetylene–like molecule. A typical time scale for this process is $\tau^{\rm dest} = 1/k_{\rm C}^{\rm UV}$ where $k_{\rm C}^{\rm UV}$ represents the rate for photoabstraction of carbon discussed in Sect. 2.3. The equilibrium of ionization is typically reached on a timescale $\tau^{\rm ion} = 1/(k^{\rm ion} + n_{\rm e} k^{\rm rec})$ where $k^{\rm ion}$ and $k^{\rm rec}$ are the rates of ionization and electron recombination presented in the previous section. Hydrogenation equilibrium occurs on a timescale $\tau^{\rm hyd} = 1/(k_{\rm H}^{\rm UV} + n_{<{\rm H}>} k^{\rm hyd} + n_{<{\rm H}>} k^{\rm abst})$ where $k_{\rm H}^{\rm UV}$, $k^{\rm hyd}$ and $k^{\rm abst}$ are the rates for photoabstraction of hydrogen, hydrogenation and chemical abstraction, respectively. Using the numerical values obtained in the previous sections shows that in all situations $\tau^{\rm dest}$ is at least one order of magnitude larger than $\tau^{\rm hyd}$ and $\tau^{\rm ion}$. This ensures the existence of the equilibrium.

To determine the ionization and the hydrogenation state of a given PAH *(P)* with $N_{\rm C}$ carbon atoms and $N_{\rm H}^{\circ}$ hydrogen atoms in its non dehydrogenated form, we consider an ensemble of $N_{\rm PAH}$ PAHs *(P)*. For the N_i neutral PAHs *(P)* bearing i hydrogen atoms we introduce n_i, the concentration relative to the total number of PAHs ($n_i = N_i/N_{\rm PAH}$). We also define c_i the concentration of the corresponding PAH cations. At equilibrium, the concentrations remain constant and we consequently infer the following conservation equations[1]:

$$\begin{aligned}
&\text{for the neutrals} \quad i = 0, 1, 2, ..., N_{\rm H}^{\circ}\,, \\
\frac{dn_i}{dt} \;=\;& n_{i-1}\left(n_{\rm H} k_{{\rm H}\;i-1}^{\rm hyd\;(n)}\right) + \\
& n_{i+1}\left(\chi k_{{\rm H}\;i+1}^{\rm UV\;(n)} + n_{\rm H} k_{{\rm H}\;i+1}^{\rm abs\;(n)}\right) + \\
& n_{i+2}\left(\chi k_{{\rm H_2}\;i+2}^{\rm UV\;(n)}\right) + c_i\left(n_{\rm e} k^{\rm rec}\right) - \\
& n_i \sum k^{(n)} \;=\; 0\,, \qquad (13)
\end{aligned}$$

$$\begin{aligned}
&\text{for the cations} \quad i = 0, 1, 2, ..., N_{\rm H}^{\circ}\,, \\
\frac{dc_i}{dt} \;=\;& c_{i-1}\left(n_{\rm H} k_{{\rm H}\;i-1}^{\rm hyd\;(c)}\right) + \\
& c_{i+1}\left(\chi k_{{\rm H}\;i+1}^{\rm UV\;(c)} + n_{\rm H} k_{{\rm H}\;i+1}^{\rm abs\;(c)}\right) + \\
& c_{i+2}\left(\chi k_{{\rm H_2}\;i+2}^{\rm UV\;(c)}\right) + n_{i-1}\left(n_{\rm H+} k_{{\rm H+}\;i-1}^{\rm hyd\;(n)}\right) + \\
& n_i\left(\chi k_i^{\rm ion}\right) + n_{i+1}\left(n_{\rm H+} k_{{\rm H+}\;i+1}^{\rm abs\;(n)}\right) - \\
& c_i \sum k^{(c)} \;=\; 0\,, \qquad (14)
\end{aligned}$$

where

[1] In the following equations for i=0, i=$N_{\rm H}^{\circ}$-1 and i=$N_{\rm H}^{\circ}$ the terms corresponding to i-1, i+2, i+1 and i+2 respectively have to be set equal to zero.

Table 4. Physical properties of some astrophysical regions showing the UIR bands.

medium	Object	$n_{<\mathrm{H}>}^{(1)}$ (cm^{-3})	$n_{\mathrm{e}}^{(2)}$ (cm^{-3})	T (K)	$\chi^{(3)}$
Planetary nebula	NGC 7027$^{(a)}$	7 (4)$^{(b)}$	7 (1)	5 (2)	4.6 (5)
Photodissociation region	Orion Bar$^{(c)}$	1 (5)$^{(d)}$	3 (1)	5 (2)	4.3 (3)
Reflection Nebula	NGC 7023$^{(e)}$	4 (3)$^{(f)}$	1 (0)	2.5 (2)	2.5 (3)
Galactic nucleus	M82$^{(g)}$	1 (4)$^{(h)}$	3 (0)	2.5 (2)	2.9 (3)
HI region	Galactic plane$^{(i)}$	5 (1)$^{(j)}$	2 (-2)	8 (1)	1 (0)
Diffuse warm medium	Galactic plane$^{(i)}$	5 (-1)$^{(j)}$	4 (-3)	8 (3)	1 (0)

(1) total density of hydrogen nuclei, (2) electron density, (3) scaling factor to be multiplied to the photon flux of Gondhalekar *et al.* (1980) to describe the UV radiation field .
References to the observations and physical conditions (a) Cohen *et al.* (1986), (b) Allamandola *et al.* (1989), (c) Bregman *et al.* (1989), (d) Tielens and Hollenbach (1985a, 1985b), (e) Sellgren *et al.* (1985), (f) Chokshi *et al.* (1988), (g) Willner *et al.* (1977), (h) Wolfire *et al.* (1988), (i) Giard *et al.* (1988) and (j) Spitzer (1978)

$$\begin{aligned}\sum k^{(n)} &= n_{\mathrm{H}} k_{\mathrm{H}}^{\mathrm{hyd}}{}_{i}^{(\mathrm{n})} + n_{\mathrm{H+}} k_{\mathrm{H+}}^{\mathrm{hyd}}{}_{i}^{(\mathrm{n})} + n_{\mathrm{H}} k_{\mathrm{H}}^{\mathrm{abs}}{}_{i}^{(\mathrm{n})} + \\ &\quad n_{\mathrm{H+}} k_{\mathrm{H+}}^{\mathrm{abs}}{}_{i}^{(\mathrm{n})} + \chi k_{\mathrm{H}}^{\mathrm{UV}}{}_{i}^{(\mathrm{n})} + \chi k_{\mathrm{H_2}}^{\mathrm{UV}}{}_{i}^{(\mathrm{n})} + \chi k_{i}^{\mathrm{ion}} \,, \\ \sum k^{(c)} &= n_{\mathrm{H}} k_{\mathrm{H}}^{\mathrm{hyd}}{}_{i}^{(\mathrm{c})} + n_{\mathrm{H}} k_{\mathrm{H}}^{\mathrm{abs}}{}_{i}^{(\mathrm{c})} + \chi k_{\mathrm{H}}^{\mathrm{UV}}{}_{i}^{(\mathrm{c})} + \\ &\quad \chi k_{\mathrm{H_2}}^{\mathrm{UV}}{}_{i}^{(\mathrm{c})} + n_{\mathrm{e}} k^{\mathrm{rec}} \,. \end{aligned} \quad (15)$$

In Eqs. (13), (14) and (15), n_{X} represents the density of species X, and $k_{\mathrm{X}}^{p}{}_{i}^{(s)}$ the rate for process p involving the species X and a PAH (P) with i hydrogen atoms in state (s) where s can be neutral (n) or cationic (c). Equations (13) and (14) constitute a system of $2(N_{\mathrm{H}}^{\circ}+1)$ equations with $2(N_{\mathrm{H}}^{\circ}+1)$ unknowns (the n_i and c_i). These equations are not independent because each of them can be deduced from the sum of all the others. To solve the system, we therefore replace one of the equations by the conservation equation:

$$\sum_{i=0}^{N_{\mathrm{H}}^{\circ}} n_i + \sum_{i=0}^{N_{\mathrm{H}}^{\circ}} c_i = 1 \,. \quad (16)$$

The solution of this system provides the distribution of PAHs *(P)* in its different hydrogenated and ionized forms at equilibrium.

As in paper I we apply our calculations to some astrophysical media where the IR emission bands attributed to PAHs have been seen. These media are presented in Table 4 together with their physical properties and the references to the observations. The results of the calculations are discussed in the two next sections, which concern the ionization and hydrogenation states of PAHs, respectively.

3.2.2. Ionization state of PAHs in the ISM

Léger & d'Hendecourt (1985) and Verstraete *et al.* (1990) have already discussed the state of ionization of PAHs. We likewise introduce the ionization fraction α_{ion} to describe the state of ionization of an assembly of PAHs

$$\alpha_{\mathrm{ion}} = \frac{n_{\mathrm{ion}}}{n_{\mathrm{ion}} + n_{\mathrm{molecule}}} \,, \quad (17)$$

where n_{ion} represents the density of PAH cations and n_{molecule} the density of neutral molecules. With the notations of Sect. 3.2.1 we obtain for α_{ion} the following expression:

$$\alpha_{\mathrm{ion}} = \sum_{i=0}^{N_{\mathrm{H}}^{\circ}} c_i \,. \quad (18)$$

We present in Fig. 7 the ionization fractions calculated for the astrophysical media of Table 4 as a function of the molecular size. The results are in good agreement with the calculations of Verstraete *et al.* (1990) who have studied α_{ion} in the case of a PAH molecule containing 80 carbon atoms, assuming however a sticking probability of 1 for the electron recombination process. Figure 7 shows a slight increase of the ionization fraction with the molecular size. It also reveals a large dependence of the ionization fraction with the physical parameters.

In order to study more precisely this dependence, we use an alternative expression of α_{ion} obtained by summing the relations (13) and using the conservation Eq. (16). After some algebra, one obtains:

$$\alpha_{\mathrm{ion}} = \frac{k_{<\mathrm{i}>}^{\mathrm{ion}} + \frac{n_{\mathrm{H+}}}{\chi} k_{<\mathrm{i}>}^{\mathrm{hyd}}}{k_{<\mathrm{i}>}^{\mathrm{ion}} + \frac{n_{\mathrm{H+}}}{\chi} k_{<\mathrm{i}>}^{\mathrm{hyd}} + \frac{n_{e}}{\chi} k^{\mathrm{rec}}(T)} \,, \quad (19)$$

where we have defined mean rates over the hydrogenation states:

$$k_{<\mathrm{i}>}^{\mathrm{ion}} = \frac{\sum n_i \, k_i^{\mathrm{ion}}}{\sum n_i} \,, \quad (20)$$

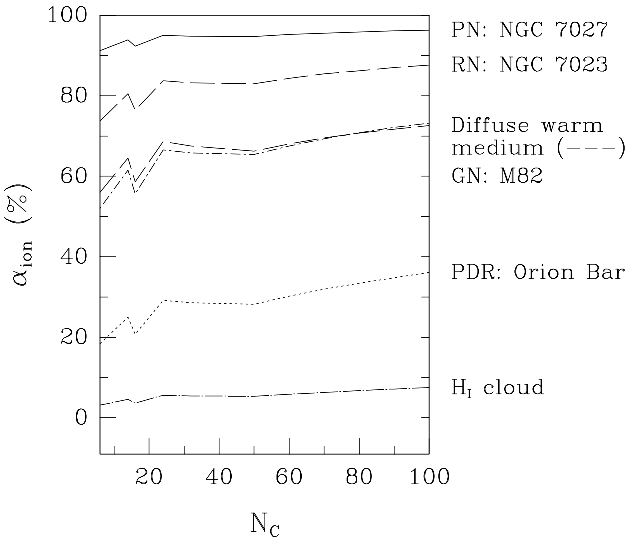

Fig. 7. Ionization fraction of PAHs for various astrophysical media as a function of the molecular size. (PN: Planetary Nebula, RN: Reflection Nebula, GN: Galactic Nucleus, PDR Photodissociation Region)

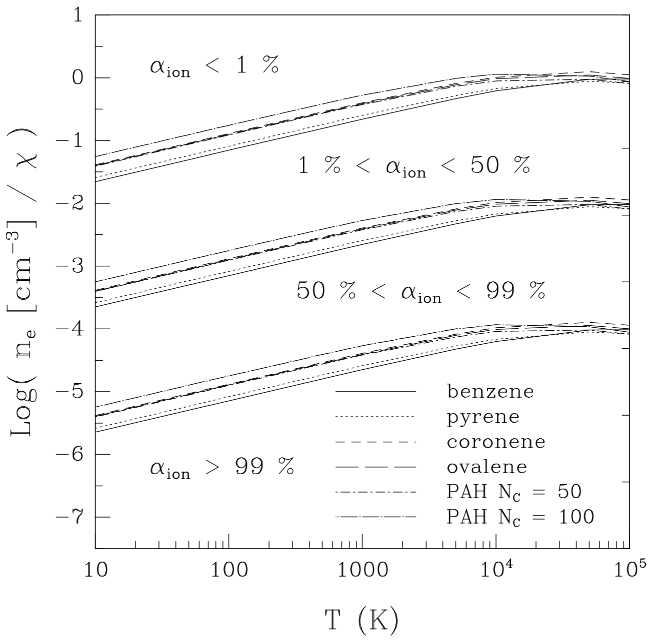

Fig. 8. Ionization equilibrium curves in the plane $T, log(n_e/\chi)$ for various values of α_{ion} and for various PAHs.

$$k^{\rm hyd}_{<\rm i>} = \frac{\sum n_i \; k^{\rm hyd}_i}{\sum n_i} \; .$$

In most regions showing the UIR bands, $n_{\rm H+}$ is low enough so that one can omit the term $n_{H+}k^{\rm hyd}/\chi$ in Eq. (19)[1]. Under these circumstances $\alpha_{\rm ion}$ can be written as a function of T and $n_{\rm e}/\chi$ for each PAH. In order to have some insight into the influence of those parameters, we represent $\alpha_{\rm ion}$ in the plane T, $\log(n_{\rm e}/\chi)$. Figure 8 shows the results obtained for the values 0.01, 0.50 and 0.99 of the ionization fraction and for various PAHs. We observe again in Fig. 8 that all PAHs have approximatly the same ionization fraction. For a given temperature the ionization fraction decreases with the electron density (because the rate of recombination decreases) and increases with the radiation field intensity (because the ionization rate increases). More quantitatively, a decrease of the intensity of the UV-field by two orders of magnitude or an increase of the electron density by two orders of magnitude could make the ionization fraction drop from 99 % to 50 %; the same variations could cause a drop from 50 % to 1 %. The dependence on the temperature is relatively less important. More precisely, we deduce from Fig. 8 that full ionization ($\alpha_{\rm ion} \geq 99\%$) of PAHs is achieved for a ratio $n_{\rm e}/\chi$ lower than $n_{\rm e}/\chi_{99\%} = 10^{-6}\, T^{0.42}$ cm^{-3}. Neutral PAHs are to be found in large amounts ($\alpha_{ion} \leq 1\%$) in regions having a ratio n_e/χ greater than $n_e/\chi_{1\%} = 10^{-2}\, T^{0.42}$ cm^{-3}.

A consequence of this sensitivity of the ionization fraction to the various physical parameters is that any attempt to determine the ionization state of PAHs will be very dependent on the quality of the evaluation of the temperature, photon flux and electron density. Moreover, as has already been seen for the media of Table 4, the values of $n_{\rm e}/\chi$ observed in the regions where the UIR bands have been seen range from 10^{-5} cm^{-3} to 10^{-1} cm^{-3}. Consequently all the values of $\alpha_{\rm ion}$ may be encountered in regions showing the UIR bands.

3.2.3. Hydrogenation state of PAHs

Figure 9 shows the distribution of hydrogen atoms obtained for benzene and coronene type molecules and cations in two different media. Some differences can be observed between ionic and neutral PAHs for a given PAH in a given environment, between the two PAHs in a given environment, and also between a PAH in two different media. To simplify the discussion, we therefore define a mean hydrogen coverage for cations and for molecules by the following expression:

for the neutrals,

$$\alpha_{\rm H}(n) = \sum_{i=0}^{N_{\rm H}^{\circ}} \frac{i}{N_{\rm H}^{\circ}}\; n_i \; ,$$

for the cations,

[1] In HII regions the term $n_{\rm H+}k^{\rm hyd}/\chi$ accounting for the PAH ionization via reaction with H^+ has to be taken into account. However, in these media $n_e \simeq n_{\rm H+}$ and the dominant process electron recombination, so that $\alpha_{\rm ion} \ll 1$ (see Sect. 3.2.4).

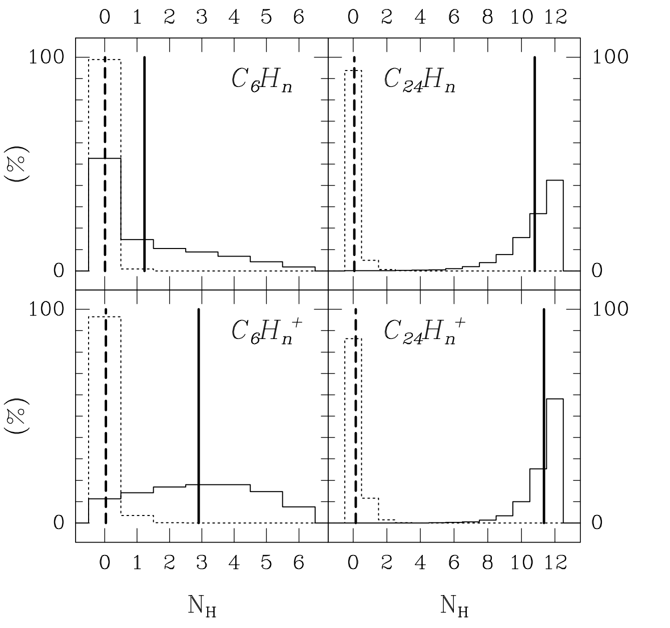

Fig. 9. Distribution of PAHs according to their number of hydrogen atoms. The solid lines refer to the case of NGC 7027, the dashed ones to the PDR of the Orion Bar. The bold bins represent the mean number of hydrogen atoms $\bar{N}_{\rm H} = \alpha_{\rm H} N_{\rm H}^{\circ}$.

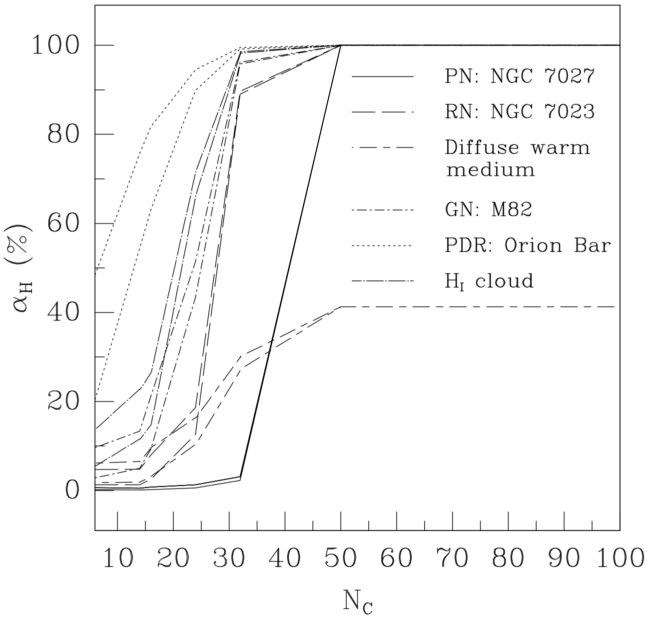

Fig. 10. Hydrogen coverage of PAHs in some astrophysical media as a function of molecular size. For each medium the two curves represent $\alpha_H(n)$ and $\alpha_{\rm H}(c)$, hydrogen coverage for neutrals (lower curve) and for cations (upper curve), respectively.

$$\alpha_{\rm H}(c) = \sum_{i=0}^{N_{\rm H}^{\circ}} \frac{i}{N_{\rm H}^{\circ}}\, c_i \ . \tag{21}$$

We have presented in Fig. 9 $\bar{N}_{\rm H} = \alpha_{\rm H} N_{\rm H}^{\circ}$ the mean number of hydrogen atoms borne by the PAHs. In the cases of total dehydrogenation and of high hydrogen content $\bar{N}_{\rm H}$ corresponds to the number of hydrogen atoms borne by the majority of PAHs. For medium values of $\alpha_{\rm H}$ all states of hydrogenation can be observed and $\bar{N}_{\rm H}$ (respectively $\alpha_{\rm H}$) loses its representative meaning and must really be understood as a mean value.

Figure 10 shows the hydrogen coverage of PAH cations and molecules as a function of the molecular size in the media of Table 4. Because of their larger hydrogenation rate cations have larger hydrogen coverage than the neutrals but this difference tends to diminish with molecular size. In all the astrophysical environments investigated, $\alpha_{\rm H}$ increases with size up to a plateau for PAHs having more than 50 carbon atoms. The existence of this plateau can be understood from Eqs. (13) and (14) when one neglects the rate of photodissociation leading to loss of hydrogen, which considerably drops for large molecules. The remaining terms do not markedly depend on the molecular size, so that the value of $\alpha_{\rm H}$ in this plateau region therefore depends only on the temperature. The evolution of $\alpha_{\rm H}$ with temperature for large PAHs is shown in Fig. 11. Up to 1000 K, $\alpha_{\rm H}$ is equal to 100 %. Since the chemical abstraction reactions are dominant for $T > 2000$ K, the hydrogen coverage drops in this temperature range, reaching a value of a few per cent for $T > 10^4$ K. Such temperatures can be reached in HII regions and shocked-regions.

Since the 3.3 μm band of the UIR features has also been observed in the HII region of NGC 7027, we also investigate the influence of the ionization fraction of hydrogen ξ defined as $\xi = n_{\rm H+}/n_{<\rm H>}$ where $n_{\rm H+}$ and $n_{<\rm H>}$ represent the proton density and the total density of hydrogen nuclei, respectively. For the calculations the electron density is set equal to:

$$\begin{aligned} n_{\rm e} &= n_{\rm H+} + n_{\rm M+} \\ &\simeq \xi\, n_{<\rm H>} + 5.10^{-4}\, n_{<\rm H>} \ , \end{aligned} \tag{22}$$

where M represent the metallic species C, Si, S, Fe assumed to be present according to their solar abundances and fully ionized in only one ionization state.

As suggested from the study of ionization, a representation of the state of equilibrium in the plane T , $\log(n_{<\rm H>}/\chi)$ may provide a interesting view of the influence of the physical parameters on the hydrogen coverage. Figure 12 shows the locations of the curves for $\alpha_{\rm H}$ equal to 1 %, 50 % and 99 % in the case of an ensemble of pyrene molecules and of pyrene cations for regions with various values of the ionization fraction of atomic hydrogen ξ. From Fig. 12 it can be seen that **(i)** a full hydrogen content of pyrene PAH ($\alpha_{\rm H} > 99$ %) is only possible

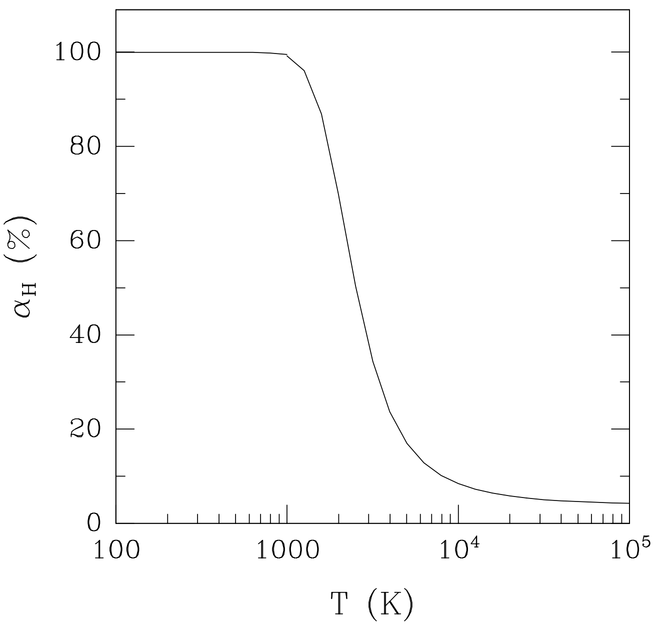

Fig. 11. Hydrogen coverage of large PAHs ($N_C > 50$) as a function of temperature.

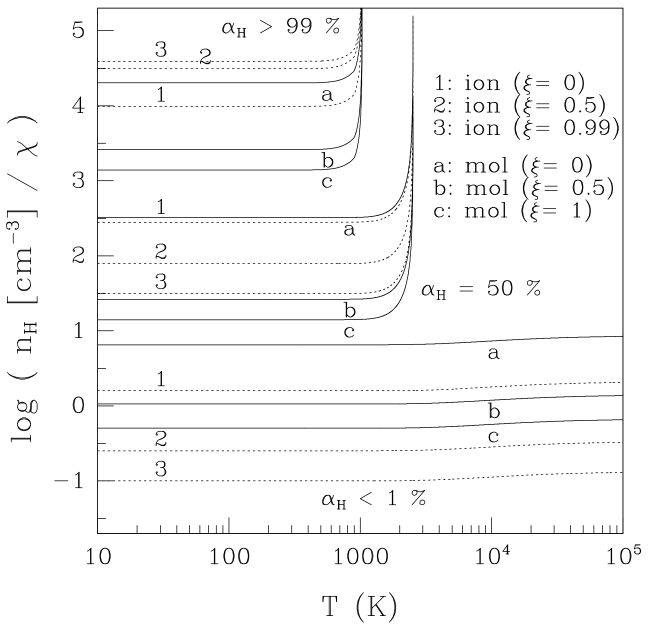

Fig. 12. Hydrogenation equilibrium curves in the plane T , $log(n_{<\mathrm{H}>}/\chi)$ for pyrene molecules and cations in region with various values of the ionization fraction of atomic hydrogen ξ, and for three hydrogen coverage regimes, α_{H} = 1, 50, 99 %.

for a temperature lower than 1000 K and a high value of $n_{<\mathrm{H}>}/\chi$ ($n_{<\mathrm{H}>}/\chi > 10^4$ cm^{-3} at $T = 100$ K for pyrene cations and $\xi = 0$); **(ii)** a total dehydrogenation ($\alpha_{\mathrm{H}} < 1$ %) is reached for sufficiently low values of $n_{<\mathrm{H}>}/\chi$ whatever the value of the temperature ($n_{<\mathrm{H}>}/\chi < 2$ cm^{-3} at $T = 100$ K for pyrene cations and $\xi = 0$); **(iii)** a given state of hydrogen content, that is to say a given value of α_{H}, is obtained for various ionization fractions of atomic hydrogen and states of ionization of PAHs at different values of $n_{<\mathrm{H}>}/\chi$. A total dehydrogenation of pyrene cations in a highly ionized region requires a low value of $n_{<\mathrm{H}>}/\chi$ (curve 3 in Fig. 12), whereas the higher value is needed in the case of pyrene molecules in a region with $\xi = 0$ (curve a in Fig. 12). A medium value of $n_{<\mathrm{H}>}/\chi$ is that required by pyrene cations in a region with $\xi = 0$ (curve 1 in Fig. 12).

In order to investigate the effect of the molecular size on situations **(i)**, **(ii)** and **(iii)** we have plotted in Fig. 13 the locations of the curves α_{H} equal 1% and 99 % for various PAH cations in a region with $\xi = 0$ (these curves are equivalent to the curve 1 in Fig. 12). We observe in Fig. 13 that for a given value of α_{H} the curves of all PAHs can be deduced from any one of them by displacement along the y axis. This leads to three interesting consequences: **(I)** the previous observations **(i)**, **(ii)** and **(iii)** can be applied to each PAH with the corresponding values of $n_{<\mathrm{H}>}/\chi$. The larger the PAH, the lower the value of $n_{<\mathrm{H}>}/\chi$ needed to reach a given state of hydrogenation and the narrower the region in the plane T , $\log(n_{<\mathrm{H}>}/\chi)$ where $1\% < \alpha_{\mathrm{H}} < 99\%$; **(II)** to have a given value of α_{H}, the temperature must not be greater than a maximum value which is the same for all PAHs and is consequently equal to that for large PAHs given in Fig. 11 ; **(III)** the media where the UIR bands have been seen have all values of $n_{<\mathrm{H}>}/\chi$ ranging between 10^{-1} and 10^2 cm^{-3}, and temperatures lower than some 10^3 K. We deduce from Figs. 12 and 13 that, in these media, PAHs having less than 50 carbon atoms are partially dehydrogenated, whereas larger PAHs have their full hydrogen content.

3.2.4. Relation between hydrogenation and ionization

It was stated in Sect. 3.1.2 that hydrogenation of PAH cations is more rapid than that of their corresponding molecules. However, it can be seen by comparison of Figs. 7 and 10 that hydrogenation of small PAHs is more efficient in the media where the PAH ionization fraction is lower. The explanation for this phenomenon is that hydrogenation increases with the hydrogen density (see Figs. 12 and 13) whereas ionization decreases with the electron density (see Fig. 8). As the electron density practically varies as a linear function of the hydrogen density in the regions of interest here (see Eq. (22)), high hydrogen coverage of small PAHs are always related to low ionization fraction of PAHs. This result is confirmed in Fig. 14, where ionization fraction and hydrogen coverage of some PAHs are plotted as a function of $n_{<\mathrm{H}>}/\chi$ for a typical region

Table 5. Typical times for the photodestruction of PAHs in some astrophysical media (unit = year).

Medium	benzene			pyrene			ovalene		
	deh. ion(1)	mol.(2)	mean(3)	deh. ion(1)	mol.(2)	mean(3)	deh. ion(1)	mol.(2)	mean(3)
NGC 7027	1.2 (-5)	4.7 (-4)	1.8 (-5)	6.0 (-6)	9.7 (-4)	1.7 (-5)	1.1 (-5)	1.4 (-2)	1.1 (-4)
Orion Bar	1.3 (-3)	5.0 (-2)	2.1 (-2)	6.4 (-2)	1.6 (-1)	1.2 (-1)	1.2 (-3)	1.5 (0)	1.2 (0)
NGC 7023	2.3 (-3)	8.6 (-2)	9.0 (-3)	1.1 (-3)	1.8 (-1)	1.5 (-2)	2.1 (-3)	2.6 (0)	7.0 (-1)
M82	2.0 (-3)	7.4 (-2)	1.2 (-2)	9.6 (-4)	1.5 (-1)	2.4 (-2)	1.8 (-3)	2.3 (0)	9.9 (-1)
HI region	5.7 (0)	2.2 (2)	3.6 (1)	2.8 (0)	4.5 (2)	8.2 (1)	5.2 (0)	6.5 (3)	5.8 (3)
Diffuse warm medium	5.7 (0)	2.2 (2)	2.5 (1)	2.8 (0)	4.5 (2)	3.9 (1)	5.2 (0)	6.5 (3)	3.7 (2)

(1) totally dehydrogenated PAH cation, (2) PAH molecule, (3) average value taking into account all hydrogen and ionized forms of the PAH according to their concentration.

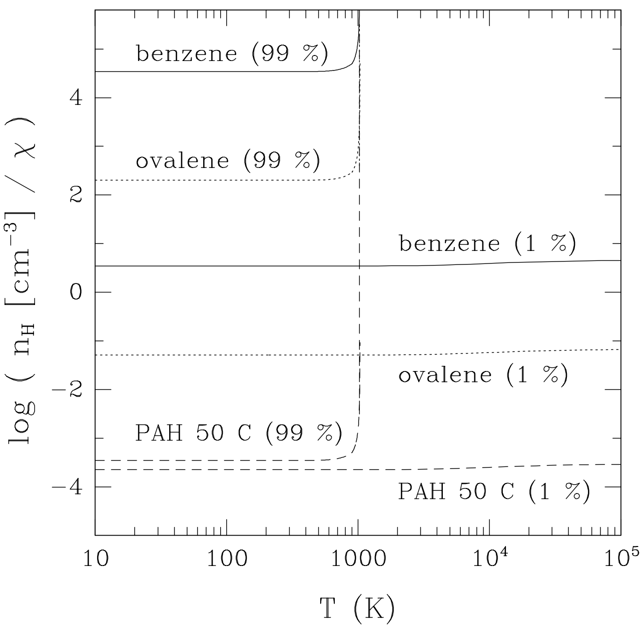

Fig. 13. Hydrogenation equilibrium curves in the plane T, $log(n_{<H>}/\chi)$ for various PAHs cations in a region with an ionization fraction of atomic hydrogen $\xi = 0$,and for two hydrogen coverage regimes, $\alpha_H = 1$, 99 %.

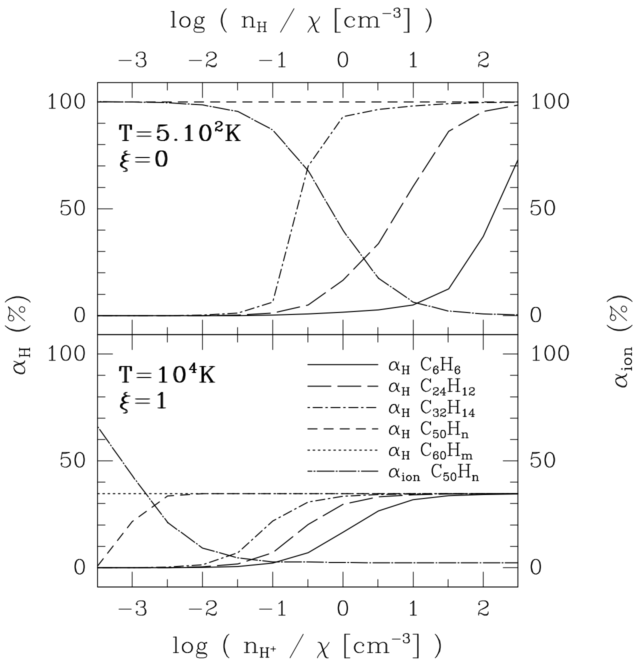

Fig. 14. Ionization fraction and hydrogen coverage of some PAH molecules in a typical region showing the UIR bands (upper diagram) and in a HII region (lower diagram).

showing the UIR bands (T = 500 K and $\xi = 0$) and in a typical HII region ($T = 10^4$ K and $\xi = 1$).

4. Astrophysical implications

In paper I we introduced two characteristic times in the study of the photostability of PAHs molecules in an astrophysical medium: τ^{UV}, the time for photodestruction via loss of carbon and τ^{gr}, the time for growth by accretion of carbon particles. These times are defined as follows:

$$\tau^{\mathrm{UV}} = \frac{1}{k_{\mathrm{C}}^{\mathrm{UV}}},$$

$$\tau^{\mathrm{gr}} = \frac{1}{n_{<\mathrm{C}>}\, k_{\mathrm{C}}^{\mathrm{acc}}} \simeq 10^{12} \left(\frac{n_{<\mathrm{C}>}}{1\ \mathrm{cm}^{-3}}\right)^{-1} \ \mathrm{sec}, \qquad (23)$$

where $k_{\mathrm{C}}^{\mathrm{UV}}$ is the value for the loss of carbon from a PAH and where $n_{<\mathrm{C}>}$ and $k_{\mathrm{C}}^{\mathrm{acc}}$ represent the density of carbon particles (carbon atoms or cations) and their rate of accretion onto PAHs. It was established in paper I that PAHs having less than 50 carbon atoms have a characteristic time of photodissociation $\tau^{\rm UV}$ smaller than the time for growth $\tau^{\rm gr}$, and that they are consequently destroyed within a time $\tau^{\rm UV}$. We have seen here that in astrophysical environments showing the UIR bands these PAHs are probably ionized and partially dehydrogenated. Under these conditions the values of $\tau^{\rm UV}$ and $\tau^{\rm gr}$ are different from those of PAH molecules. However, we assume here that the time for accretion of carbon particles can still be used. This timescale should indeed account for accretion of both carbon atoms and carbon ions and we have therefore used a mean value in paper I for all these processes. This time may be smaller for partially dehydrogenated PAHs because of their radical sites, but also greater for PAH cations because of the Coulomb repulsion with C^+. We therefore keep the value of paper I for the present discussion. On the other hand, the results of Sect. 2.3 have shown that the rates for photodissociation of ionized and dehydrogenated PAHs are much greater than the corresponding rates for full hydrogen content molecules. The times $\tau^{\rm UV}$ are consequently lower. As in paper I, we therefore conclude that $\tau^{\rm UV} < \tau^{gr}$ for small PAHs ($N_{\rm C} < 50$) in the media where the UIR bands are seen.

These results confirm the destruction of small PAHs. Moreover, we conclude here that destruction of these small PAHs is more rapid than that calculated in paper I. To illustrate this result, we have presented in Table 5 the times of destruction of some small PAHs in their molecular and totally dehydrogenated ionized form and also for a mean state corresponding to the average ionization and hydrogen content of PAHs in the considered medium. To take into account the state of hydrogenation and ionization of PAHs we have calculated the rate for photodissociation of carbon as follows:

$$k_{\rm C}^{\rm UV} = \sum_{i=0}^{N_{\rm H}^{\circ}} \chi \; n_i \; k_{{\rm C}\;\,i}^{{\rm UV}\;(n)} + \sum_{i=0}^{N_{\rm H}^{\circ}} \chi \; c_i \; k_{{\rm C}\;\,i}^{{\rm UV}\;(c)} \; , \tag{24}$$

with the notations of Sect. 3.2.1. The values of the lifetimes in Table 5 put into question the existence of small free PAHs in the regions showing the UIR bands. Unless it can be shown that a more rapid formation process, such as erosion of hydrogenated amorphous carbon (HAC)(Duley 1987, 1988), could justify their presence in these environments it is indeed doubtful whether free small PAHs could be the carriers of the UIR bands as proposed by Allamandola *et al.* (1985), Geballe *et al.* (1989), Woodward *et al.* (1989) and more recently by Duley & Jones (1990). However, as has been suggested by Duley (1987, 1988), Duley & Jones (1990) and Allamandola (1991), IR emission could originate from PAHs loosely bonded to interstellar dust, which could therefore be more stable against photodissociation than free PAHs.

Because of their greater size, large PAHs ($N_{\rm C} > 50$) also resist the UV radiation field of the ISM. We have indeed found that in regions where the UIR bands are seen, chemical abstraction is more efficient than photodissociation in removing hydrogen from large PAHs. However, chemical sputtering competes with hydrogenation and can lead to dehydrogenation of PAHs only in regions with a temperature higher than 2000 K. Such situations may be found in HII regions and in shocked regions (Brown *et al.* 1989, Flower *et al.* 1990).

Chemical sputtering leading to a loss of carbon atoms is also probably a important factor of destruction of PAHs. Omont (1986) has estimated that this would mainly occur by reactions between C^+ and PAH molecules. The ratio of the condensation yield to the sputtering yield should however not be greater than 10 %. This means that PAHs having a photodissociation rate equal or larger than the accretion rate are more likely to be destroyed via UV photodissociation. In order to determine the size of the smaller PAHs which may survive the radiation field we therefore compare the time for accretion $\tau^{\rm gr}$ to the time $\tau^{\rm UV}$ for photodestruction, as in paper I. For representational convenience we have plotted in Fig. 15 $k^{\rm acc}/n_{<{\rm C}>} = 1/\tau^{\rm gr} n_{<{\rm C}>} = 10^{-12}$ s^{-1}cm^3 and $k_{\rm C}^{\rm UV}/n_{<{\rm C}>} = 1/\tau^{\rm UV} n_{<{\rm C}>}$ for various astrophysical media. From Fig. 15 we observe that surviving PAHs in all these media have more than 40 carbon atoms. The smallest size is obtained for the Photodissociation Region of the Orion Bar and for the HI cloud where PAHs have a relatively high hydrogen content (see Sect. 3.2.3). On the other hand, in regions with a low hydrogen coverage small PAHs are more rapidly destroyed and the size of the smaller surviving PAHs is slightly greater: 50 carbon atoms in NGC 7027 and 55 carbon atoms in the warm diffuse medium. These conclusions are, however, not very different from those of paper I because the PAHs surviving the UV radiations do not undergo a massive loss of hydrogen in the regions showing the UIR bands and have therefore similar rates as those of the PAH molecules considered in paper I.

The determination of the hydrogen content and ionization states of PAHs have shown some mutual influence between hydrogenation and ionization processes. Progress could be made to better analyze this coupling. At the present time it is not possible to correctly evaluate the rate of electron recombination for PAHs in various states of hydrogen content. Experimental data in this area would be of interest for astrophysicists because it is needed for precise estimation of the ionization fraction of PAHs. We note also that the results presented here have been obtained under the assumption of ionization and hydrogenation equilibrium. A dynamical calculation of the competing processes of ionization, hydrogenation and photodestruction of PAHs may provide some interesting new results. A forthcoming paper will propose a procedure to simulate the evolution of the hydrogen coverage and ionization fraction of PAHs in an astrophysical environment.

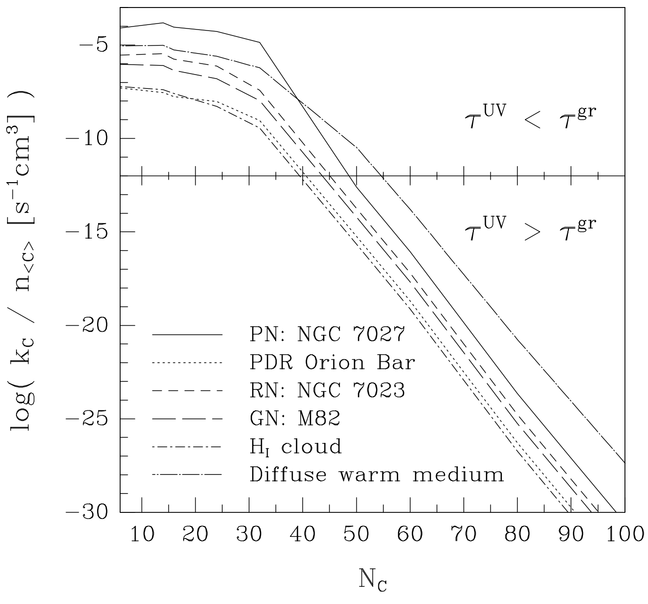

Fig. 15. Determination of the minimal size of surviving PAHs in various astrophysical environments.

5. Conclusion

A large fraction of interstellar PAHs are ionized and partially dehydrogenated. In the regions of the ISM where the UIR bands have been observed (reflection nebulae, planetary nebulae, HII regions, active galactic nuclei...) the ionization fraction of PAHs may indeed largely vary and it depends mainly on the intensity of the UV field and on the electron density. On the other hand, the hydrogen content is relatively similar in all the previously mentioned media. The hydrogen coverage increases with molecular size up to a value of 100 % for PAHs having more than 50 carbon atoms. For temperatures higher than some 10^3 K this size limit decreases because of the chemical abstraction of hydrogen. A high hydrogen coverage of small PAHs is favored in regions where the ionization fraction of PAHs is relatively low, whereas marked dehydrogenation can occur at high temperatures and low hydrogen densities, which induce a high ionization fraction.

An extension of the model for interstellar PAHs of paper I to the case of PAH cations and dehydrogenated PAHs has allowed the calculation of the corresponding photodissociation rates. It is found that cations and partially dehydrogenated PAHs are less stable than their parent molecules. Cation rates are on average 5 times larger than the rates of the corresponding molecules calculated in paper I. For partially dehydrogenated PAHs differences are much larger and they increase with both molecular size and degree of dehydrogenation. For a totally dehydrogenated coronene molecule there is a two orders of magnitude difference. This indicates that PAHs with less than 50 carbon atoms probably do not survive more than a year in the regions of high UV radiations where the UIR are seen. If these PAHs are really the carriers of the UIR bands it may be necessary to find a very efficient process for their formation. Most likely small PAHs emit while they are still bound in PAH clusters such as HAC. Large PAHs with more than 50 carbon atoms may also be the carriers of the UIR bands because their rates of photodissociation are lower that the rate for carbon accretion in the regions showing the UIR emission bands. Since it is now well documented that PAHs could form in circumstellar winds of late type stars (Keller & Sedlmayr 1983; Keller 1987; Frenklach & Feigelson 1989; Cherchneff *et al.* 1992; Cadwell *et al.* 1994), it would be of great interest to precisely study their growth at least up to a size of 50 carbon atoms.

Acknowlegements. T. Allain acknowledges MESR (Ministère de l'Enseignement Supérieur et de la Recherche, France) for a doctoral fellowship (n° 92342).

References

Abouelaziz H., Gomet J .C., Pasquerault D., Rowe B. R., Mitchell J. B. A., 1993, J. Chem. Phys, 99, 237

Allain T., Leach S., Sedlmayr E., 1995, A&A submitted

Allamandola L. J., 1991, International School of Physics "Enrico Fermi", Course CXI, Solid State Astrophysics, page 1, Bussoletti E. and Strazzulla G.: North–Holland.

Allamandola L. J., Tielens A. G. G. M., Barker J. R., 1985, ApJ 290, L25

Allamandola L. J., Tielens A. G. G. M., Barker J. R., 1987, Polycyclic Aromatic Hydrocarbons and Astrophysics, volume 191, page 255. Léger, A., d'Hendecourt, L. B. and Boccara N., (eds.)Dordrecht: Reidel

Allamandola L. J., Tielens A. G. G. M., Barker J. R., 1989, ApJS 71, 733

Barlow M. J., Silk J., 1977, ApJ 215, 800

Bregman J. D., Allamandola L. J., Tielens A. G. G. M., Geballe T. R., Witteborn F. C., 1989, ApJ 344, 791

Brown P. D., Duley W. W., Jones A. P., Williams D. A., 1989, MNRAS 241, 753

Cadwell B. J., Wang H., Feigelson E. D., Frenklach M., 1994, ApJ 429, 285

Cherchneff I., Barker J. R., Tielens A. G. G. M., 1992, ApJ 401, 269

Chokshi A., Tielens A. G. G. M., Werner M. W., Castelaz M. W., 1988, ApJ 334, 803

Cohen M., Allamandola L., Tielens A. G. G. M., Bregman J., Simpson J. P., Witteborn F. C., Wooden D., Rank D., 1986, ApJ 302, 737

Draine B. T., 1979, ApJ 230, 106

Duley W. W., 1987,MNRAS 229,203

Duley W. W., 1988,MNRAS 234,61P

Duley W. W., Jones A. P., 1990, ApJ 351, L49

Dunbar R. C., 1986, Chem. Phys. Let. 125, 543

Flower D. R., Heck L., Pineau des Forets G., Millar T. J., 1990, MNRAS 242, 512

Frenklach M., Clary D. W., Gardiner W. C. Jr., Stein S. E., 1985, 20 th. Symp. Int. on Combustion, page 887, Pittsburgh: The Combustion Institute
Frenklach M., Feigelson E. D., 1989, ApJ 341, 372
Geballe T. R., Tielens A. G. G. M., Allamandola L. J., Moorhouse A., Brand P. W. J. L., 1989, ApJ 341, 278
Giard M., Pajot F., Lamarre J. M., Serra G., Caux E., Gispert R., Léger A., Rouan D., 1988, A&A 201, L1
Giard M., Bernard J. P., Normand P., Rouan D., 1994, A&A 291, 239
Gillet F. C., Forrest W. J., Merril K. M., 1977, ApJ 183,87
Goeres A., 1993, Stellar Evolution and Interstellar Matter, p. 165, Astron. Gesellschaft, Klage Ed.
Gondhalekar P. M., Phillips A. P., Wilson R., 1980, A&A 128, 212
Jochims H. W., Rühl E., Baumgärtel H., Tobita S., Leach S., 1994a, ApJ 420, 307
Jochims H. W., Baumgärtel H., Leach S., 1994b, in preparation
Keller R., Sedlmayr E., 1983, Mitt. d. Astron. Ges., 60, 312.
Keller R., 1987, Polycyclic Aromatic Hydrocarbons and Astrophysics, volume 191, page 387. Léger, A., d'Hendecourt, L. B. and Boccara, N., (eds.) Dordrecht: Reidel
Kiefer J. H. Mizerka L. J., Patel M. R., Wei H. C., 1985, J. Phys. Chem. 89, 2013
Klippenstein S. J., Faulk J. D., Dunbar R. C., 1993, J. Chem. Phys. 98, 243
Leach S., 1986, J. Elect. Spectr. Rel. Phen. 41, 427
Leach S., 1987, Polycyclic Aromatic Hydrocarbons and Astrophysics, volume 191, page 99. Léger, A., d'Hendecourt, L. B. and Boccara, N. , (eds) Dordrecht: Reidel
Leach S., Eland J. H. D., Price S. D., 1989, J. Phys. Chem. 93, 7583
Lee W., Wdowiak T. J., 1993a, ApJ 410, L127
Lee W., Wdowiak T. J., 1993b, ApJ 417, L49
Léger A., d'Hendecourt L., 1985, A&A 146, 81
Léger A., Puget J. L., 1984, A&A 137, L5
Léger A., Boissel P., Désert F. X., d'Hendecourt L., 1989a, A&A 213, 351
Léger A., d'Hendecourt L., Defourneau D., 1989b, A&A 216, 148
Mathis J. S., Metzger P. S., Panagia N., 1978, A&A 128, 212
Nicovich J. M., Ravishankara A. R., 1984, J. Phys. Chem. 88, 2234
Omont A., 1986, A&A 164, 159
Pulay P., Fogarasi G., Boggs J. E., 1981, J. Chem. Phys. 74, 3999
Salama F., Allamandola L. J., 1991, J. Chem. Phys. 94, 6964
Salama F., Allamandola L. J., 1992, ApJ 395, 301
Sellgren K., Allamandola L. J., Bregman J. D., Werner M. W., Wooden D. H., 1985, ApJ 217, 416
Spitzer L., 1978, Physical Processes in the Interstellar Medium, Wiley, New–York
Tielens A. G. G. M., Allamandola L. J., Barker J. R., Cohen M, 1987, Polycyclic Aromatic Hydrocarbons and Astrophysics, volume 191, page 273. Léger, A., d'Hendecourt, L. B. and Boccara, N. , (eds.) Dordrecht: Reidel
Tielens A. G. G. M., Hollenbach D. J., 1985a, ApJ 291, 722
Tielens A. G. G. M., Hollenbach D. J., 1985b, ApJ 291, 747
van der Zwet G. P., Allamandola L. J., 1985, A&A 146, 76
Tobita S., Leach S., Jochims H. W., Rühl E., Illenberger E., Baumgärtel H., 1994, Can. J. Phys. 72 (in press)
Verstraete L., Léger A., 1992, A&A 266, 513
Verstraete L., Léger A., d'Hendecourt L., Dutuit O., Defourneau D., 1990, A&A 237, 436
Willner S., Soifer B. T., Russell R. W., Joyce R. R., Gillet F. C., 1977, ApJ 217, L121
Wolfire M., Tielens A. G. G. M., Hollenbach D. J., 1988, ApJ 358, 116
Woodward C. E., Pipher J. L., Shure M., Forrest W. J., Sellgren K, 1989, ApJ 342,860

This article was processed by the author using Springer-Verlag LaTeX A&A style file *L-AA* version 3.